JVSTA Journal of Vacuum Science & Technology A

Design and qualification of an UHV system for operation on sounding rockets

Jens Grosse, Stephan Tobias Seidel, Dennis Becker, Maike Diana Lachmann, Marco Scharringhausen, Claus Braxmaier, and Ernst Maria Rasel

Citation: Journal of Vacuum Science & Technology A **34**, 031606 (2016); doi: 10.1116/1.4947583
View online: http://dx.doi.org/10.1116/1.4947583
View Table of Contents: http://scitation.aip.org/content/avs/journal/jvsta/34/3?ver=pdfcov
Published by the AVS: Science & Technology of Materials, Interfaces, and Processing

Design and qualification of an UHV system for operation on sounding rockets

Jens Grosse[a)]
Center of Applied Space Technology and Microgravity (ZARM), University of Bremen, Bremen, 28359, Germany and German Aerospace Center (DLR) Bremen, Bremen, 28359, Germany

Stephan Tobias Seidel,[b)] Dennis Becker, and Maike Diana Lachmann
Institute of Quantum Optics, Leibniz University Hanover, Hanover, 30167, Germany

Marco Scharringhausen
German Aerospace Center (DLR) Bremen, Bremen, 28359, Germany

Claus Braxmaier
Center of Applied Space Technology and Microgravity (ZARM), University of Bremen, Bremen, 28359, Germany and German Aerospace Center (DLR) Bremen, Bremen, 28359, Germany

Ernst Maria Rasel
Institute of Quantum Optics, Leibniz University Hanover, Hanover, 30167, Bremen

(Received 17 February 2016; accepted 14 April 2016; published 11 May 2016)

The sounding rocket mission MAIUS-1 has the objective to create the first Bose–Einstein condensate in space; therefore, its scientific payload is a complete cold atom experiment built to be launched on a VSB-30 sounding rocket. An essential part of the setup is an ultrahigh vacuum system needed in order to sufficiently suppress interactions of the cooled atoms with the residual background gas. Contrary to vacuum systems on missions aboard satellites or the international space station, the required vacuum environment has to be reached within 47 s after motor burn-out. This paper contains a detailed description of the MAIUS-1 vacuum system, as well as a description of its qualification process for the operation under vibrational loads of up to 8.1 g_{RMS} (where RMS is root mean square). Even though a pressure rise dependent on the level of vibration was observed, the design presented herein is capable of regaining a pressure of below 5×10^{-10} mbar in less than 40 s when tested at 5.4 g_{RMS}. To the authors' best knowledge, it is the first UHV system qualified for operation on a sounding rocket. © *2016 American Vacuum Society*. [http://dx.doi.org/10.1116/1.4947583]

I. INTRODUCTION

The scientific objective of the MAIUS-1 mission is to demonstrate the feasibility of creating Bose–Einstein condensates and performing atom interferometry in space.[1,2] In order to achieve this goal, a vacuum pressure of less than 5×10^{-10} mbar in the experiment chamber was defined as the design criterion.

The MAIUS-1 experiment will be launched on a VSB-30 sounding rocket operated by the DLR Mobile Rocket Base (MORABA).[3] It will lift the payload to an apogee of 238 km, providing approximately 360 s of microgravity. During the burn phase of approximately 44 s, the motors will cause accelerations[4] of up to 13 g and vibrational loads[5] of 1.8 g_{RMS} (where RMS is root mean square). The friction of the atmosphere causes decelerations of more than 20 g during re-entry. Although the payload is recovered using parachutes, shock loads of up to 100 g are expected during landing.

Because of the harsh sounding rocket environment, it is a mechanical requirement that the vacuum system parts are capable of carrying static loads of 100 g. Moreover, the system and its components have to be qualified in random vibration tests at levels of up to 8.1 g_{RMS} as described in Sec. III B.

In addition to the requirements imposed by the launcher, the system has to deliver the electrical currents as well as the laser light needed for the experiments to the place of the atoms. This requires 36 electrical connections into the vacuum system and 12 optical viewports. A system meeting all requirements listed above has been developed and its design is described in Sec. II. The system has intensively been tested, and the test methods as well as their results are given in Sec. III.

II. VACUUM SYSTEM DESIGN

The MAIUS-1 scientific payload consists of four systems: the battery and power distribution system, the electronic system, the laser system, and the physics package. All instruments of the MAIUS-1 payload are mounted to standardized platforms, each connected to the rocket hull by six brackets. These brackets contain a passive vibration isolation, which has been developed for MAIUS-1.[6]

The vacuum system of MAIUS-1 is part of the physics package, which is mounted between two of these platforms. The vacuum section is divided into the pumping system above the upper platform and the two experiment chambers between the upper and lower platform, as shown in Fig. 1.

Inside the preparation chamber, a cooled atomic beam of Rubidium 87 is formed in a two dimensional magneto-optical trap[7] and transferred into the science chamber. In the science chamber, the atoms are caught in a three dimensional

[a)]Electronic mail: jens.grosse@dlr.de
[b)]Present address: German Aerospace Center (DLR) Oberpfaffenhofen, Münchener Straße 20, 82234 Weßling.

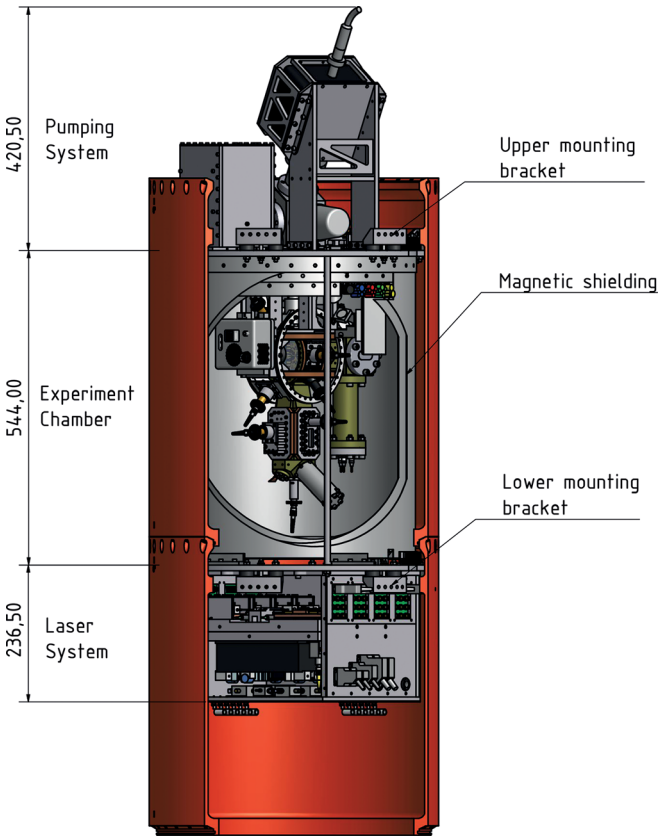

FIG. 1. (Color online) Physics package and laser system assembly mounted into two hull segments of the MAIUS-1 payload. The physics package splits into two parts the pumping system and the experiment chamber enclosed by a magnetic shielding. Reprinted from Proceedings of the 66th International Astronautical Congress.

magneto-optical trap and subsequently cooled to Bose–Einstein condensation. The magnetic fields needed for cooling of the atoms are formed by an atom chip placed inside the science chamber in combination with a set of external coils. The selection of appropriate materials is essential for the successful design of the vacuum system. For the material of the MAIUS-1 system, five criteria have been identified: A low magnetic susceptibility, a low outgassing rate, a low density, a high yield strength, and a high hardness.

As experiments with Bose–Einstein condensates are sensitive to magnetic fields, external fields as well as fields induced by the vacuum chamber itself could disturb the measurements. While a three layer magnetic shielding[8] with a shielding factor of over 1000 reduces the external fields to below 100 nT, the use of materials with a low magnitude of magnetic susceptibility minimizes the induced fields in the chamber walls.

A low outgassing rate is needed to achieve the required vacuum quality. Therefore, a careful preparation of all surfaces in contact with the vacuum is essential.

A low density is required to achieve a system with a low mass. For a sounding rocket payload, this is essential, because a high mass will lower the apogee and therefore the time in microgravity.

A high yield strength and hardness of the material is necessary for a high capacity of the chamber for carrying mechanical loads. Moreover, both properties will allow a reliable use of standard CF seals at the chamber.

Table I lists the three candidates considered for the material of the vacuum chamber and their properties. Titanium Grade 5 has been preferred to aluminum as material for the vacuum chambers, because CF-knife edges made of titanium are common state-of-the-art and have been used in several chamber designs. However, it has to be noted that aluminum knife edges have been introduced as component-of-the-shelf[13] after the completion of the design phase of the vacuum chambers. Stainless steel (1.4404) was not selected for the chamber, due to its comparably high magnetic susceptibility and higher density. However, it is used for vacuum components outside the magnetic shielding, because of its lower cost.

A. Pumping system

Figure 2 shows that the components of the MAIUS-1 pumping system are arranged around a single stainless steel cube equipped with four CF40 ports and two CF16 ports. One CF16 port is establishing the connection to the roughening pump with a copper pinch-off tube. The opposing CF40 port is closed with a blind flange.

A turbomolecular pumping station with a capacity of 67 l s^{-1} is used as roughening pump. The roughening pump is connected with one copper pinch-off tube each to the 2D magneto-optical trap (MOT) chamber and to the pumping system during preparation and bake-out of the vacuum system. The bake-out temperature is limited to 100 °C due to the indium seals used at the windows (compare Sec. II B). Thus, the bake-out time is comparably long (3–4 weeks). After bake-out, the pressure stagnates at around 5×10^{-10} mbar, which is the base pressure of the turbopump. At this point, the pinch-off tubes are closed using a hydraulic tool. During the pinch-off procedure, the copper tube is hermetically sealed by hydraulic jaws with a pressure of 700 bar. This process is irreversible; thus, the MAIUS-1 pumping system has to resume pumping independently after pinch-off to compensate for residual outgassing of components inside the vacuum or gas entering the system through small leaks. The pumping rate needed to maintain the vacuum quality is

TABLE I. Properties of materials considered for the vacuum chambers.

Material	Outgassing rate (Ref. 9) (10^{-10} mbar l cm^{-2} s^{-1})	Magnetic susceptibility	Density (g/cm^3)	Yield strength (MPa)
Titanium grade 5 (Ti6Al4V) (Ref. 10)	4.9–24.5	5×10^{-5}	4.45	910
Stainless steal (1.4404) (Ref. 11)	18.0	7×10^{-1}	7.98	360
Aluminum (EN AW 7075) (Ref. 12)	8.0	2.2×10^{-5}	2.8	220–460

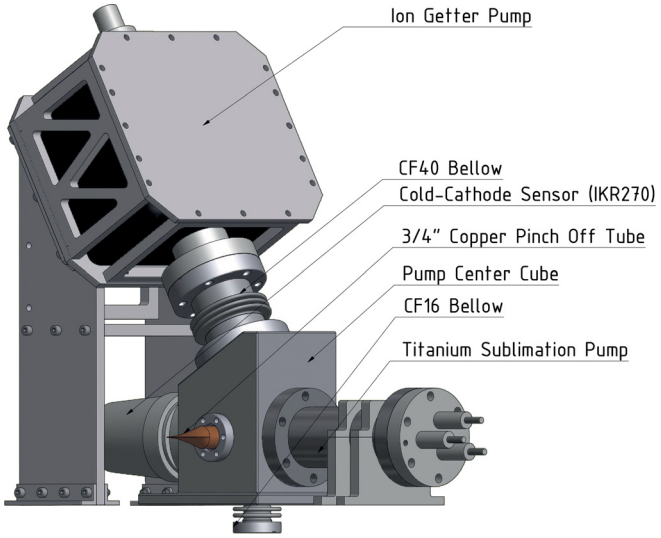

FIG. 2. (Color online) MAIUS-1 pumping system components assembled around a stainless steel center cube. The connection to the experiment chamber is established by a CF16 bellow mounted to the center cube from beneath. Reprinted from Proceedings of the 66th International Astronautical Congress.

generated by a commercial titanium sublimation pump ST22 manufactured by VG Scienta and an ion-getter pump VacIon 20Plus by Varian/Agilent. Both pumps are connected to a CF 40 port of the center cube. The titanium sublimation pump ST22 sublimes titanium from one of its three filaments, which gets deposits at the walls of the surrounding tube. The formed layer of titanium is capable of gettering gas molecules from the vacuum system. The pump in MAIUS-1 has been modified by the supplier to be shorter than the standard pump measuring only 105.5 mm. As shown in Fig. 3, the pump is installed in a custom-made CF40 stainless steel pipe with a length of 125 mm, offering an internal surface of 149.22 cm^2 for the titanium to deposit on.

The pipe is equipped with a M38 × 1.5 thread at one end to install a mesh, which prevents fragments of the filaments from floating into the science chamber during microgravity phase if the filaments would break as a result of the strong accelerations during lift off.

Unfortunately, the mesh will also reduce the effective pumping speed by blocking the molecular flow into the tube. The conductance of the sieve is limiting the pumping speed for all gases to roughly 18 l s^{-1}, as shown in Table II.

The pumping rate of the titanium layer will be reduced by 50% in 17 h and to 10% in 7 days at a pressure of 1×10^{-10} mbar;[15] however, this will only result in a reduction of 3.03% behind the sieve, because the conductivity is limiting the effective pumping speed.

In addition to the titanium sublimation pump, an Agilent VacIon 20 Plus[16] noble diode ion getter pump is connected to the center cube by a CF40 bellow. The ion-getter pump is the only device capable of pumping inert gases, such as noble gases or methane, once the roughening pump is separated from the MAIUS-1 vacuum system. Thus, it is essential to reach the desired pressures. At a pressure of 1×10^{-10} mbar, the pump will provide a pumping speed[16] of 25 l s^{-1} for nitrogen and 11 l s^{-1} for noble gases. These rates reduce to 15 l s^{-1} and (8 l s^{-1} if the pump is saturated.[16] Saturation will take 1 year[15] at a pressure of 1×10^{-10} mbar.

The pressure of the vacuum system is monitored by a Pfeiffer IKR 270 cold cathode vacuum gauge capable of measuring pressures between 1×10^{-11} and 1×10^{-3} mbar. It is directly mounted to the remaining CF40 port at the center cube.

The port for the connection to the experiment chamber is hidden below the cube. This allows us to use a straight pipe to connect the two regions of the vacuum system, which will maximize the effective pumping speeds at the 3D chamber. Since the experiment chamber itself is rigidly mounted to the instrument platform, a bellow has to be added to the tube to prevent mechanical stress on the seals due to the mounting situation.

B. Experiment chamber

The experiment chamber consists of the science chamber (3D-MOT), the preparation chamber [$2D^+$-MOT,[7] and the

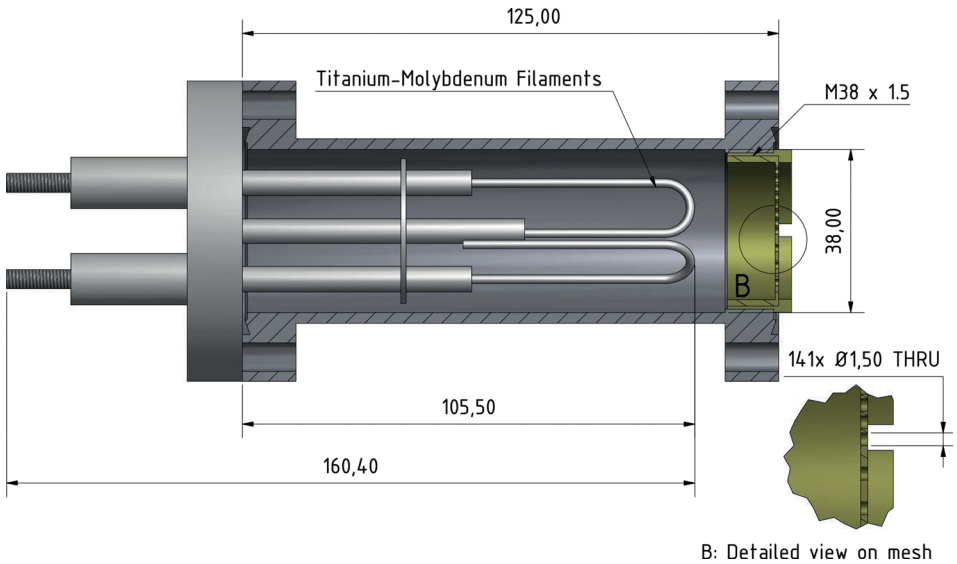

FIG. 3. (Color online) Titanium sublimation pump setup used in MAIUS-1. Reprinted from Proceedings of the 66th International Astronautical Congress.

TABLE II. Pumping speed of MAIUS-1 titanium sublimation pump setup.

Gas	Pumping rate (Ref. 14) ($l\,s^{-1}\,cm^{-2}$)	Effective pumping rate ($l\,s^{-1}$)
H_2	3	18.28
H_2O	3	18.28
CO	9	18.79
N_2	4	18.47
O_2	2	17.91
CO_2	8	18.76
CH_4	0	0

atom chip cube, as shown in Fig. 4. All three parts are manufactured from Grade 5 titanium (Ti6Al4V).

The atom chip mount is equipped with five CF40 ports. Four ports are used to mount commercial DSUB feedthroughs, which are connected to the atom chip using Kapton insulated wires. To compensate for the outgassing[17] of the wires and the glue used to assemble the chip, a second titanium sublimation pump is mounted to the remaining CF40 port in close proximity of the wires and the chip.

The atom chip cube is mechanically connected to the science chamber by a flange, which is sealed using indium wire. The science chamber is equipped with six view ports with a diameter of 30 mm and a seventh viewport with a diameter of 87 mm, as shown in Fig. 4. These viewports are needed to shine in laser light for magneto-optical trapping of the atoms. Sealing of the BK7-glass windows is achieved by using indium wire, which allows a more compact chamber design compared to commercial CF-sealed viewports.

A CF16 port at the science chamber establishes the connection to the pumping system center cube as mentioned in Sec. II A. Opposite to the CF16 port, the preparation chamber is brazed to the science chamber using a thin silver foil. This procedure establishes a solid and rigid connection with a tensile strength of 456.25 MPa as demonstrated in one-dimensional tensile tests. The use of a foil ensures a brazed connection over the entire contact surface of the two parts, which is required to avoid virtual leaks.

As shown in Fig. 4, a differential pumping stage (DPS) is installed between both chambers to allow to operate the preparation chamber with a high rubidium partial pressure needed for fast creation of Bose–Einstein condensates, without influencing the vacuum quality in the science chamber. The high rubidium partial pressure causes an absolute pressure around 1×10^{-9} mbar in the preparation chamber. The conductance of the DPS of below 0.0551 s^{-1} results in a pressure gradient of 2 orders of magnitude between the science and preparation chamber.[2]

The preparation chamber is equipped with four rectangular indium-sealed viewports. Moreover, two CF16 ports are located at the bottom of the chamber. One of the CF16 ports is used to connect the rubidium source to the chamber, while a copper pinch off tube is mounted to the other one.

As mentioned in Sec. II A, this copper pinch off tube is connected to the roughening pump during vacuum preparation to avoid pumping the preparation chamber through the differential pumping stage, which would be inefficient due to the small conductance.

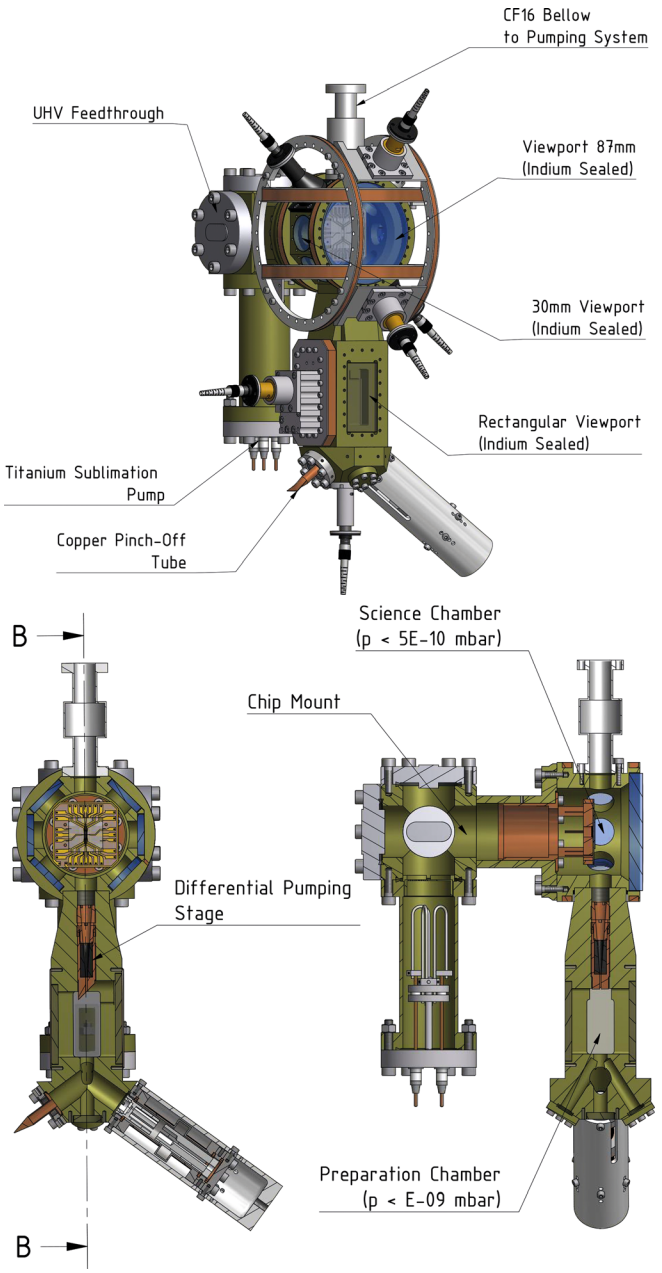

FIG. 4. (Color online) MAIUS-1 experiment chamber assembly overview and section view through two perpendicular planes. Reprinted from Proceedings of the 66th International Astronautical Congress.

III. VACUUM SYSTEM QUALIFICATION

A. Vacuum system performance

The overall vacuum system demonstrated pressures as low as 6.7×10^{-11} mbar at 22 °C ambient temperature with newly activated titanium sublimation pumps and shortly after bake-out (assuming an unsaturated ion-getter pump). The typical pressure after a year of operation is 1.8×10^{-10} mbar. A monthly firing of the titanium sublimation pump is sufficient to maintain this pressure.

The effective pumping speed of all three pumps for nitrogen at an absolute pressure of 1×10^{-10} mbar at the science chamber, preparation chamber, and the pump cube has been approximated by calculating the conductance of every component in the path between the pump and the location of interest.

Assuming a saturated ion-getter pump and a recently fired titanium sublimation pump, the effective pumping speed at the pump cube is 29.581 s^{-1}. The effective pumping speed of the pumping system is reduced to 2.931 s^{-1} at the science chamber by the small conductance of the CF16 pipe connecting the pumping system with chamber. Thus, the effective pumping speed at the science chamber is dominated by the second titanium sublimation pump, which provides 11.91 s^{-1} at the center of the chamber. The pumping speed at the preparation pump is negligible due to the small conductance of the differential pumping stage.

B. Vibrational tests

The qualification procedure for components launched on a VSB-30 rocket includes a random vibration test in all three axes for 60 s. The load level is dependent upon the test specimen. Single instruments are first tested at a qualification level. Subsequently, the systems of the payload or functional groups are tested at an acceptance level. Ultimately, the entire payload is tested in flight configuration at an acceptance level once more. Table III summarizes the different test profiles. Aside from the acceptance and qualification profiles, a flight level profile was defined to predict the performance of the instruments at a vibration level close to the one measured during the first VSB30 flight.[5]

The component and system level vibration tests described in this paper have been performed at ZARM-FAB Vibration Test Lab in Bremen using a Brüel and Kjaer LDS V875 HBT 600 long-stroke exciter and an m+p VibControl control and measurement system. The test runs in X- and Y-axes are carried out on the horizontal slip table. The z-axis has been tested in the vertical operation direction of the shaker.

Before and after each random test run, sine resonance search tests at low level (0.5 g) with a sweep rate of 2 oct/min are carried out to evaluate the significant eigenfrequencies in the related axis. Deviations of the pre- and postsine resonance search test runs would indicate structural flaws resulting from the vibration test.

The components of the pumping system have been tested hard mounted in different configurations. In total, the ion getter pump and the titanium sublimation pump have been tested seven times in numerous instrument tests at 8.1 g_{RMS} in all three axes. Visual inspection of the titanium filaments and the ion pump cathode and anode revealed no damage or degradation. The pumps were functional during and after the tests. No titanium fragments were found inside the vacuum chamber, these are expected if the filaments would be damaged. Moreover, the ion-getter pump current did not show any spikes, which would occur if the electrodes would move and an arc would form between the anode and cathode.

The vacuum sensor was used in nine test runs at the qualification level. As shown in Fig. 6, the sensor tends to switch to "underrange" when operated close to the lower end of its measurement range. This phenomenon has been observed at pressures lower than 4×10^{-10} mbar and loads above 1.6 g_{RMS}. The sensor returns to reliable measurements approximately 30 s after the test run is completed. If the sensor is operated at pressures of 1×10^{-8} mbar or is exposed to a lower load level, this behavior is not observed.

The use of the vibration isolation of the instruments platforms, e.g., during the pumping system test, as shown in Fig. 5, reduces the load level by a factor of six. The damped load level is indicated by the values in brackets in Fig. 7. The data obtained from these tests with vibration isolation show a constant and reliable pressure reading.

Nevertheless, in all tests carried out, a pressure rise has been observed, which is dependent upon the load level, as shown in Figs. 6 and 7. The pressure rise is caused by external leaks. These leaks are only temporary and close once the test run is completed, which is proven, by the fact that the initial pressure is regained after the tests.

In the damped tests, it is observed that an equilibrium pressure is reached during the tests. Due to the sensor malfunction, this is not the case for the data from the undamped test. For evaluation of this data, it is important to consider

TABLE III. Vibration test profiles for MAIUS-1 hardware.

	PSD (g^2/Hz)		
Frequency (Hz)	Flight	Acceptance	Qualification
20–399	0.0003	0.002	0.0045
400–599	0.004	0.03	0.0675
600–1299	0.0003	0.002	0.0045
1300–2000	0.004	0.03	0.0675
RMS value (g)	2.0	5.4	8.1
Duration (s)	60	60	60

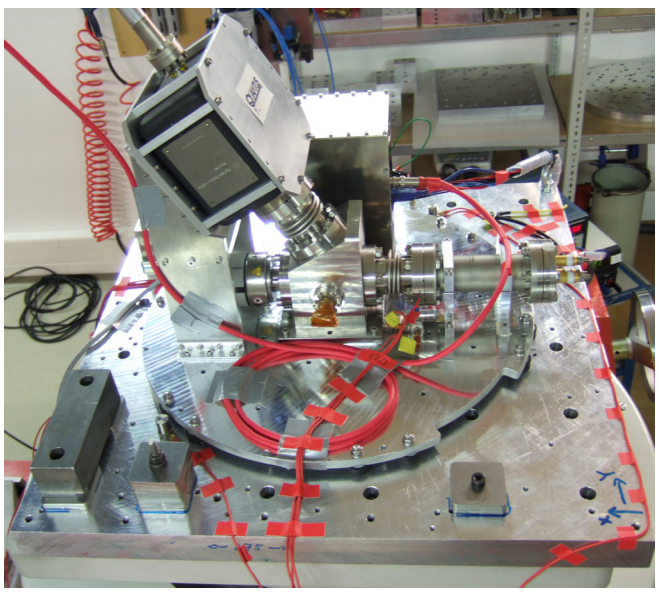

FIG. 5. (Color online) Mounting of the MAIUS-1 pumping system including instruments platform and passive vibration isolation. This configuration is similar to the flight configuration.

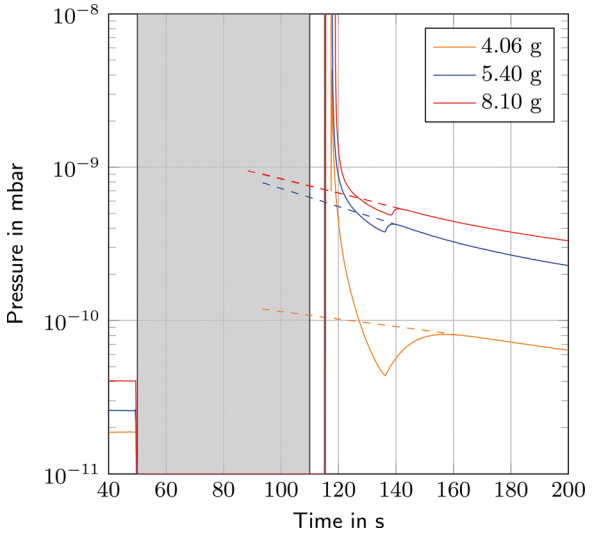

FIG. 6. (Color online) Pressure in the MAIUS-1 pumping system during z-axis random vibration tests on three different levels. The test was carried out without shock mounts. In all test runs, the sensor went to underrange, which is indicated by a pressure of 1×10^{-11} mbar. The undershooting of the actual value is a measurement artifact as it is also been observed when restarting the sensor.

the "dead-time" of the sensor of roughly 30 s. The return to reliable measurement is indicated by the dip at roughly 140 s in Fig. 6.

From the equilibrium pressure data before and during the vibrational tests presented in Table IV, the increase in leakage rate ΔQ_L is approximated. The equilibrium pressure of a vacuum system is given as[18]

$$p_{\text{end}} = \frac{Q_{\text{leak}}}{S_{\text{eff}}} + \frac{Q_{\text{des}}}{S_{\text{eff}}} + \frac{Q_{\text{diff}}}{S_{\text{eff}}} + \frac{Q_{\text{perm}}}{S_{\text{eff}}}. \quad (1)$$

This pressure is influenced by the input into the vacuum system through leaks (Q_{leak}), by desorption (Q_{des}), diffusion

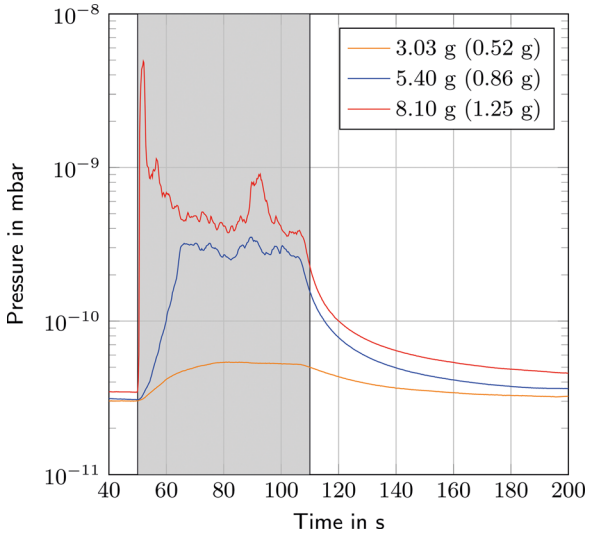

FIG. 7. (Color online) Pressure in the MAIUS-1 pumping system during z-axis random vibration tests at three different levels. The test was carried out with shock mounts. The values in brackets indicate the actual load level measured on the pumping system platform. Pressure extrapolated from reliable data.

TABLE IV. Evaluation of vibrational tests performed with the MAIUS-1 pumping system and complete vacuum system.

Load level (g_{RMS})	p_1 (t = 45)	p_2 (t = 110) (10^{-11} mbar)	p_3 (t = 140)	ΔQ_L (mbar l s^{-1})
		Pumping system		
0.52	3.01	5.23	3.52	6.57×10^{-10}
0.86	3.10	25.8	4.13	6.71×10^{-9}
1.25	3.45	37.7	5.36	1.01×10^{-8}
4.06	1.87	(11.4)	8.13	$>2.82 \times 10^{-9}$
5.40	2.62	(72.7)	32.7	$>2.07 \times 10^{-8}$
8.10	4.08	(84.2)	44.3	$>2.37 \times 10^{-8}$
		Complete vacuum system		
0.65	16.1	103	20.5	2.5×10^{-8}
1.60	16.7	790	57.0	2.28×10^{-7}

(Q_{diff}), permeation (Q_{perm}), and the effective pumping speed (S_{eff}) of the pumps at the system. Assuming that the later four factors will not change and an equilibrium pressure is reached during a test run, the increase in the leakage rate can be found from

$$\Delta Q_L = (p_{\text{end},2} - p_{\text{end},1})\, S_{\text{eff}}, \quad (2)$$

where p_1 is the equilibrium pressure before and p_2 at the end of the test run. The effective pumping speed at the pump cube close to the sensor is given in Sec. III A as 29.581 s^{-1}. This allows a good approximation of the increase in leakage rate at the pump cube, which is presented in the last column in Table IV for test runs at different load levels. As expected, the leakage rate increases with the load applied during the damped tests. Due to the sensor malfunction, no precise leakage rate could be determined for the undamped tests. For this reason, the leakage rate is approximated using the first reliable pressure measurement at $t = 140$ s to determine the pressure at the end of the test by extrapolation. This underestimates the actual pressure at this time and the rise in the leakage rate because the pumps are more efficient at higher pressures and the pressure gradient increases as shown in the undamped tests.

In addition to the pumping system test described so far, a system level test of the complete vacuum system in flight configuration has been carried out at acceptance and flight level. The setup presented in Fig. 8 also includes the vibration isolation and mounting brackets. The system is mounted to the shaker at the top and the bottom. At the top, the mounts are attached to an aluminum cylinder placed above the setup, which is not shown in Fig. 8. The vibration isolation reduces the load level to 0.65 g_{RMS} during the flight level test and to 1.6 g_{RMS} during the acceptance test. Both values have been measured at the center cube of the pumping system.

As shown in Fig. 9, the pressure rises from an initial 1.61×10^{-10} to 7.9×10^{-9} mbar, while vibrations are applied (−60 to 0 s). Afterward, the pressure recovers quickly and drops below the critical mark of 5×10^{-10} mbar after 40 s. This is within the requirements defined earlier. Thus, the time needed to regain the pressure will not reduce the time available for microgravity experiments.

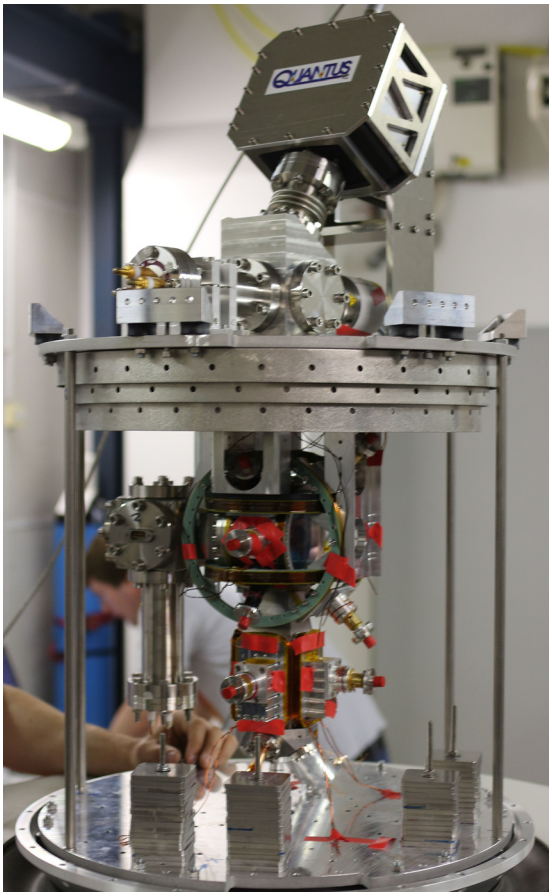

FIG. 8. (Color online) Vibration test setup for vacuum system test. The outer hull was removed from this photo.

The test at flight level results in a pressure rise to 1.03×10^{-9} mbar. The pressure drops below the 5×10^{-10} mbar mark merely 6 s after the end of the test. As the flight level represents the expected load level of vibration during the flight, the pressure is expected to recover as quickly as during this test run when the device is finally launched.

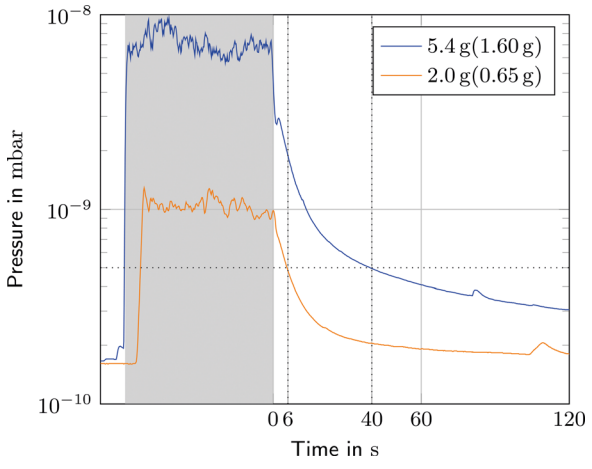

FIG. 9. (Color online) Pressure inside the MAIUS-1 vacuum system during an acceptance level showing a pressure rise to 10^{-8} mbar and a flight level test with a rise to 10^{-9} mbar. The horizontal line is the 5×10^{-10} mbar limit and the vertical dotted line the time when the limit is reached.

The leakage rates determined for the test runs are also presented in Table IV. Both values are significantly higher than those obtained from the pumping system tests at equal load levels. This is caused by the different mounting situation, which results in a higher measured load level at the center of the system and the higher number of seals in the setup.

IV. CONCLUSION

In this paper, the design of a vacuum system was presented, which is suitable for use on sounding rockets. Moreover, requirements of the cold atom experiment regarding magnetic stray fields have been fulfilled by using only materials with low magnetic susceptibility in the area of interest.

A commercial ion-getter pump Varian VacIon 20 Plus, a titanium sublimation pump VG Sienta St22 and a cold cathode gauge Pfeiffer IKR 270 have successfully been qualified in random vibration tests at levels up to 8.1 g_{RMS}.

The vacuum system shows a pressure rise, which is caused by temporal external leaks. The pressure rise is dependent upon the vibrational load level. When the vacuum system was tested in flight configuration with an initial pressure of 1.61×10^{-10} mbar, a rise to 7.9×10^{-9} mbar was observed at 5.4 g_{RMS}, while the rise was limited to 1.03×10^{-9} mbar at 2.0 $g_{RMS.}$ This corresponds to a leakage rate of 2.28×10^{-7} mbar l s^{-1} at the acceptance level and 2.5×10^{-8} mbar l s^{-1} at the flight level. It requires 40 s to regain a pressure of 5×10^{-10} mbar after a test at the acceptance level. This meets the requirements and will not reduce the available time for experiments during the microgravity phase.

ACKNOWLEDGMENTS

The MAIUS-1 mission (Materiewellen Interferometer Unter Schwerelosigkeit - Matter wave interferometer in micro-gravity) is part of the QUANTUS III Project. This project is a collaboration of Leibniz University Hanover, Humboldt University Berlin, University Hamburg, University Ulm, University Darmstadt, Ferdinand Braun Institute (FBH) Berlin, German Aerospace Center Bremen, and University Bremen. It is supported by the German Space Agency DLR with funds provided by the Federal Ministry of Economics and Technology (BMWi) under Grant No. DLR 50WM 1131-1137. The support of all team members and the funding agency is highly acknowledged by the authors.

[1]S. T. Seidel, D. Becker, J. Grosse, M. D. Lachmann, M. A. Popp, J.-B. Wang, T. Wendrich, and E. M. Rasel, *Proceedings of the 22nd ESA Symposium on European Rocket and Balloon Programmes and Related Research* (2015), pp. 309–312.
[2]S. T. Seidel, "Eine Quelle für die Interferometrie mit Bose-Einstein-Kondensaten auf Höhenforschungsraketen," Ph.D. thesis (Gottfried Wilhelm Leibniz Universität Hannover, 2014).
[3]A. Stamminger *et al.*, *Proceedings of the 22nd ESA Symposium on European Rocket and Balloon Programmes and Related Research* (2015), pp. 183–190.
[4]J. Ettl, "Post flight report TEXUS 42," Technical Report No. DLR-MR-TEXUS 42-0002, German Aerospace Center–Mobile Rocket Base, 2006.

[5]J. Ettl and E. de Barros, "Vibration evaluation of the first flight of the VSB 30," Technical Report (German Aerospace Center - Mobile Rocket Base, 2005), published in *Proceedings of the 17th ESA Symposium on European Rocket and Balloon Programmes and Related Research* (2005).
[6]J. Grossse, S. T. Seidel, M. Krutzik, T. Wendrich, A. Stamminger, and M. Scharringhausen, *Proceedings of the 22nd ESA Symposium on European Rocket and Balloon Programmes and Related Research* (2015), pp. 301–308.
[7]K. Dieckmann, R. Spreeuw, M. Weidemüller, and J. Walraven, Phys. Rev. A **58**, 3891 (1998).
[8]A. Kubelka-Lange, S. Herrmann, J. Grosse, C. Lämmerzahl, E.-M. Rasel, and C. Braxmaier, "A three-layer magnetic shielding for the MAIUS-1 mission on a sounding rocket," Rev. Sci. Instrum. (to be published).
[9]R. Elsey, Vacuum **25**, 347 (1975).
[10]ThyssenKrupp Materials Schweiz, Titan Grade 5 Werkstoff Datenblatt (2013).
[11]Deutsche Edelstahlwerke GMBH, Werkstoffdatenblatt 1.4404 (2008).
[12]Gleich Aluminium GmbH und Co KG, EN AW 7075: Technisches Datenblatt (2015).
[13]U. Bergner, S. Wolfgramm, S. Gottschall, and M. Flämmich, Vak. Forsch. Prax. **27**, 33 (2015).
[14]VG Scienta, *Operating and Maintenance Handbook ST22 Titanium Sublimation Pump Cartridge Issue B* (VG Scienta, St. Leonards on Sea, 2009).
[15]*Ion Pumps: Catalogue and Technical Notes* (Agilent Technologies, Inc., Santa Clara, 2014).
[16]Agilent Technologies, *VacIon Plus 20 Pumps: User Manual* (Agilent Technologies, Inc., Santa Clara, 2011).
[17]M. Bernardini, C. Bradaschia, H. Pan, A. Pasqualetti, R. Poggiani, G. Torelli, and Z. Zhang, "Outgassing measurements of kapton insulated cables," Technical Report No. LIGO-T960224-00-D, European Gravitational Observatory (EGO/VIRGO), 1996.
[18]*Vacuum Technology* (Pfeiffer Vacuum GmbH, Asslar, 2009).